Journal of Clinical Immunology (2019) 39:739–742
https://doi.org/10.1007/s10875-019-00667-8

LETTER TO EDITOR

LINE-1-Mediated *Alu*Ya5 Insertion Underlying Complete Autosomal Recessive IFN-γR1 Deficiency

Jérémie Rosain[1,2,3] · Caroline Deswarte[1,2] · Gonca Hancioglu[4] · Carmen Oleaga-Quintas[1,2] · Seyhan Kutlug[4] · Ibrahim Kartal[5] · Isinsu Kuzu[6] · Laurie Toullec[3] · Maud Tusseau[3] · Jean-Laurent Casanova[1,2,7,8,9] · Alisan Yildiran[4] · Jacinta Bustamante[1,2,3,7]

Received: 6 May 2019 / Accepted: 8 July 2019 / Published online: 3 August 2019

To the Editor,

Mendelian susceptibility to mycobacterial disease (MSMD) is a group of primary immunodeficiencies (PIDs) characterized by increased susceptibility to mycobacteria, including weakly virulent species such as *Bacille de Calmette et Guérin* (BCG) vaccines and environmental mycobacteria (EM), in otherwise healthy patients with no obvious immune abnormalities [1, 2]. Fifteen genes have been described as responsible for isolated or syndromic MSMD, and all these genes encode proteins involved in the production and/or action of interferon-γ (IFN-γ) [1–3]. Complete autosomal recessive (AR) IFN-γR1 deficiency is one of the most severe forms of MSMD and is characterized by a complete lack of response to IFN-γ [1]. Patients with AR IFN-γR deficiency have high plasma IFN-γ concentrations [1, 4]. Complete AR IFN-γR1 deficiency is associated with early onset disseminated infections to mycobacteria [1, 4, 5]. Severe viral infections have also been reported in rare cases [1]. Mortality is high, as 18 of the 41 patients reported to date have died [1, 4–6]. Two different forms of complete AR IFN-γR1 deficiency exist, depending on whether or not the mutant protein is expressed [1]. Complete AR IFN-γR1 deficiency has been reported in 41 patients from 33 kindreds [1, 4–6]. In total, 32 bi-allelic mutations of *IFNGR1* causing complete AR IFN-γR1 deficiency have been described [1, 4–6] including 16 single-nucleotide variants (i.e., 6 missense mutations, 4 nonsense mutations, or 6 splice-site mutations), 11 small deletions, 4 small insertions [1, 4–6], and one copy number variant (CNV) corresponding to a deletion of the entire *IFNGR1* gene [7].

The patient reported here (V.1) lives in Turkey and was born to consanguineous Turkish parents in 2013 (Fig. 1a). Both the patient's parents and his brother are healthy. The patient was vaccinated with BCG at the age of 2 months. He was hospitalized at the age of 5 months, with an ulcer at the site of BCG vaccination and a lymphadenopathy in the left axilla. Staining revealed the presence of acid-fast bacilli (AFB) in the suppurated liquid, which tested positive for *M. tuberculosis* complex by PCR. He was treated with isoniazid and rifampicin until the age of 10 months, when the

Jérémie Rosain and Caroline Deswarte contributed equally to this work.

Electronic supplementary material The online version of this article (https://doi.org/10.1007/s10875-019-00667-8) contains supplementary material, which is available to authorized users.

✉ Jérémie Rosain
jeremie.rosain@inserm.fr

✉ Jacinta Bustamante
jacinta.bustamante@inserm.fr

[1] Laboratory of Human Genetics of Infectious Diseases, Necker Branch, Inserm U1163, Necker Hospital for Sick Children, 24 boulevard du Montparnasse, Paris, EU, France

[2] Imagine Institute, Paris University, Paris, EU, France

[3] Study Center for Primary Immunodeficiencies, Necker Hospital for Sick Children, Paris, EU, France

[4] Department of Pediatric Allergy and Immunology, Faculty of Medicine, Ondokuz Mayis University, Samsun, Turkey

[5] Department of Pediatric Hematology-Oncology, Ondokuz Mayis University, Samsun, Turkey

[6] Department of Pathology, Ankara University, Ankara, Turkey

[7] St Giles Laboratory of Human Genetics of Infectious Diseases, Rockefeller Branch, Rockefeller University, New York, NY, USA

[8] Pediatric Hematology-Immunology Unit, Necker Hospital for Sick Children, AP-HP, Paris, EU, France

[9] Howard Hughes Medical Institute, New York, NY, USA

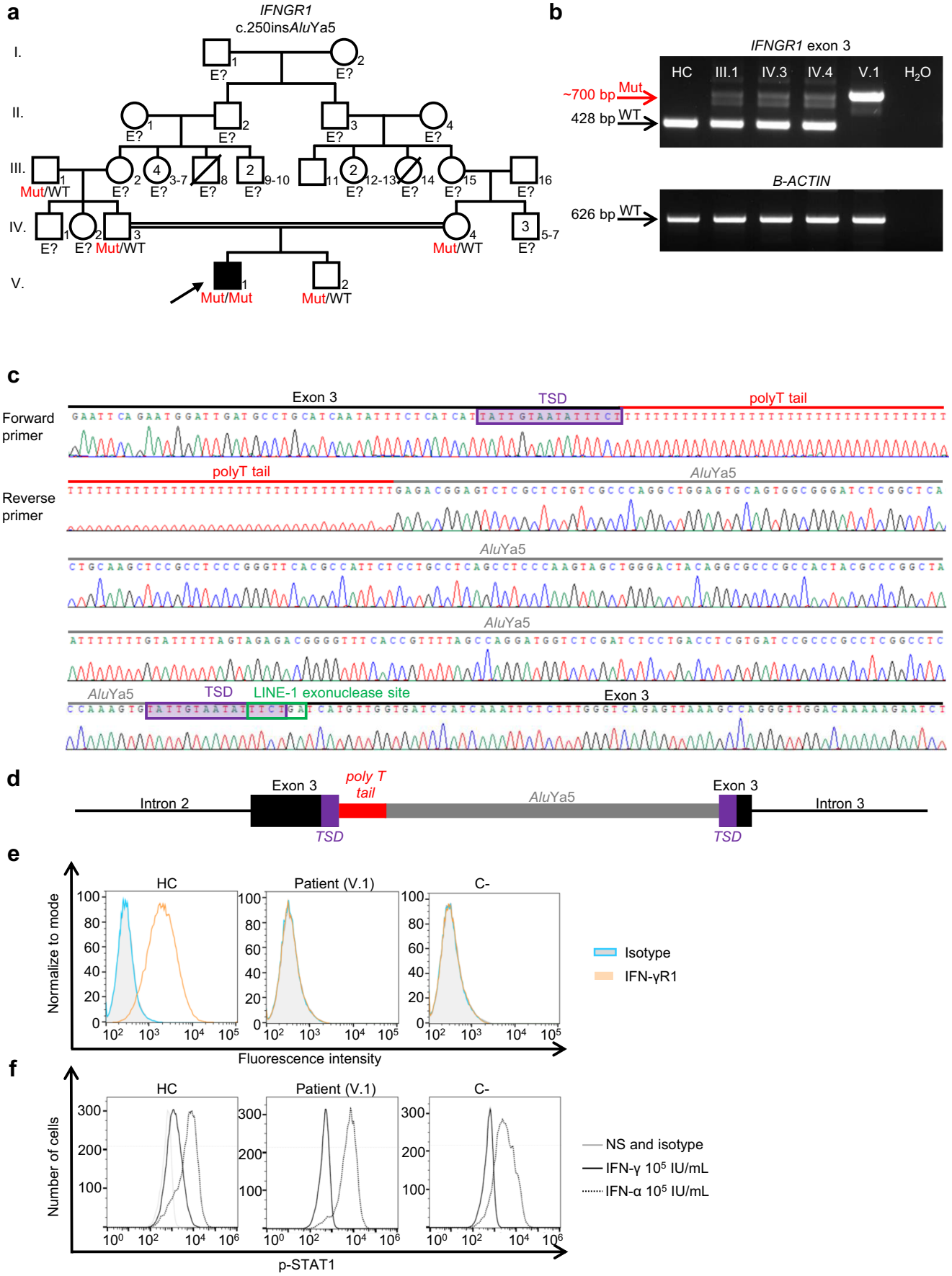
a
IFNGR1
c.250insAluYa5
I.
II.
III.
IV.
V.
E?
Mut/WT
Mut/Mut
b
IFNGR1 exon 3
HC
III.1
IV.3
IV.4
V.1
H2O
~700 bp Mut
428 bp WT
B-ACTIN
626 bp WT
c
Exon 3
TSD
polyT tail
Forward primer
Reverse primer
AluYa5
LINE-1 exonuclease site
d
Intron 2
poly T tail
Intron 3
e
HC
Patient (V.1)
C-
Normalize to mode
Fluorescence intensity
Isotype
IFN-γR1
f
Number of cells
p-STAT1
NS and isotype
IFN-γ 10⁵ IU/mL
IFN-α 10⁵ IU/mL

Fig. 1 Complete AR IFN-γR1 deficiency caused by homozygous truncated *Alu*Ya5 insertion. **a** Pedigree of the affected family. Males and females are represented by squares and circles, respectively. Each generation and each individual are designated by a Roman and an Arabic numeral, respectively. Multiple siblings are designated by numbers within the symbol. Patient with MSMD is shown as closed black symbol and indicated with an arrow. Individuals whose genetic status could not be tested are designated "E?" Mut, mutated; WT, wild-type. **b** Targeted PCR of *IFNGR1* exon 3 and of *B-ACTIN* exon 3. **c** Forward and reverse Sanger sequencing of the *IFNGR1* exon 3 PCR product from the patient (V.1). **d** Diagram of the *IFNGR1* mutation in the patient (V.1). The mutation within exon 3 consists of (i) an insertion of a thymidine repeat of ~ 35 bp (in red) and a 248 bp sequence (in gray) corresponding to a truncated reverse *Alu*Ya5 element, (ii) and a 15 bp duplication of the exon 3 sequence flanking the insertion. **e** Flow cytometry study of cell-surface IFN-γR1 expression in EBV-B cells from a healthy control (HC), the patient (V.1), and another patient with known complete AR IFN-γR1 deficiency (C-). **f** Flow cytometry study of STAT1 phosphorylation in EBV-B cells from a healthy control (HC), the patient (V.1), and another patient with known complete AR IFN-γR1 deficiency (C-)

treatment was stopped because of acute generalized exanthematous pustulosis [8]. At the age of 4 years, he presented with abdominal pain, fever, weight loss, hepatomegaly, and diarrhea on rectal enema. Positron emission tomography revealed hypermetabolic activity in multiple abdominal lymph nodes in the liver, spleen, vertebra, and femur, which was interpreted as compatible with T cell lymphoma. He received chemotherapy with prednisone and vincristine for 4 weeks, together with antimycobacterial treatment (isoniazid, rifampicin, ethambutol, and clofazimine) and regular intravenous immunoglobulin infusion. However, pathological review of the lesions provided no evidence for T cell lymphoma (Supplemental Figure 1). Chemotherapy was therefore discontinued, but antimycobacterial treatment was maintained, and the clinical response was good. Immunological assessments were performed before chemotherapy and showed the patient to be serologically negative for HIV, with normal T, B, and NK cell counts, normal T cell proliferation in response to mitogens (phytohemagglutinin and OKT3), and normal results for dihydrorhodamine tests on granulocytes.

Whole-exome sequencing (WES) of the patient revealed a rate of homozygosity of 5.5%, consistent with the consanguinity of the parents. Surprisingly, aberrant reads with non-aligned sequences both 5′ and 3′ to a 15-base pair (bp) aligned sequence were identified in exon 3 of *IFNGR1* (Supplemental Figure 2). The amplicon for exon 3 obtained from genomic DNA was larger for the patient (~ 700 bp) than for a healthy control (428 bp) (Fig. 1b). Sanger sequencing of this PCR product identified a ~ 300 bp homozygous insertion within exon 3 beginning with a stretch of ~ 35 bp T residues and flanked by a homozygous duplicated 15 bp sequence from the exon 3 (Fig. 1c, d). Alignment of the inserted sequence with RepeatMasker and Censor identified this inserted sequence as a reverse truncated *Alu*Ya5 element (Supplemental Figure 3). The mutation is referred to hereafter as c.250ins*Alu*Ya5. This *Alu* insertion was not referenced in the dbRIp repository or in the dbVar database, which includes the 2,504 structural variants from the 1000 Genomes Project. Familial segregation was analyzed by (i) haplotype analysis with microsatellites flanking the *IFNGR1* locus and a single-nucleotide polymorphism within the *IFNGR1* locus and/or (ii) targeted PCR (Fig. 1b). These analyses showed that the two parents, the paternal grandfather, and the brother carried the *Alu*Ya5 insertion in the heterozygous state (Fig. 1a and Supplemental Figure 4). Parents of the patient are consanguineous through their mother according to the known pedigree tree; however, further consanguinity loops probably go back several generations, as (i) the homozygosity rate inferred from WES is higher (5.5%) than expected (1.6%), (ii) the allele carrying the mutation is present in the paternal grandfather, and (iii) a recombination in the haplotype of the mutated allele (marker D6S262) is found across generations (Fig. 1a and Supplemental Figure 4).

We then investigated the consequences of this *Alu*Ya5 insertion, at both the RNA and protein levels. Cloning and Sanger sequencing of cDNA from the EBV-B cells of a healthy control showed that 92% of the transcripts present were wild-type whereas 8% displayed a 102 bp deletion (r.201_302del) relative to the wild-type transcript. This shorter transcript was predicted to be in frame (p.Asn70_Lys103del), and is a known alternative *IFNGR1* transcript (NM_001363527.1). Conversely, cDNA from the EBV-B cells of the patient contained 0% wild-type (WT) transcript and 90% alternative transcript r.201_302del, the remaining 10% being accounted for by three other aberrant new transcripts (Supplemental Table 1). By flow cytometry, EBV-B cells from patient did not express IFN-γR1 protein, as in a patient previously described with a complete AR IFN-γR1 deficiency (Fig. 1e). EBV-B cells from the patient also displayed no p-STAT1 induction in response to IFN-γ, as in EBV-B cells from a previously described patient with complete AR IFN-γR1 deficiency (Fig. 1f). The induction of p-STAT-1 in response to IFN-α stimulation was equivalent to that following in the healthy control (Fig. 1f). High plasma IFN-γ concentrations were detected in two separate samples (75 and 100 pg/mL, respectively). The patient had a homozygous truncated *Alu*Ya5 insertion within exon 3 of *IFNGR1*, leading in EBV-B cells to use of an alternative transcript and the complete loss of IFN-γR1 expression and function, i.e., to complete AR IFN-γR1 deficiency.

Alu elements are repetitive elements of ~ 300 bp in length that constitute 10.5% of the genome [9]. The high levels of sequence similarity between these elements can lead to genomic recombination, resulting in large deletions or duplications [10], but they can also be responsible for insertions [11]. *Alu* elements are non-autonomous mobile elements that can undergo retrotransposition mediated by a non-LTR

retrotransposon long interspersed element-1 (LINE-1) [11]. In the patient reported here, the *Alu*Ya5 element was inserted in the antisense configuration and presented a LINE-1 mediated insertion signature [11] with (i) a target site duplication of 15 bp (5′-AGAAATATTACAATA-3′), and (ii) insertion within a variant sequence (5′-TTCT/GA-3′) of the consensus (5′-TTTT/AA-3′) LINE-1 exonuclease site (Fig. 1c). *Alu*Ya5 elements are among the most active of the *Alu* subfamilies and frequently present 5′ truncation, as described in this patient [12]. *Alu* insertion can be difficult to detect at genomic level, by either WES or Sanger sequencing. Unbiased WES screening for the insertion of repetitive elements requires dedicated software [13]. Sanger sequencing may also have low sensitivity due to insufficient elongation time or because PCR and sequencing favor the WT allele in cases of heterozygous insertion. Insertion of repetitive elements can be deleterious by different mechanisms depending if occurring in translated (e.g., direct in frame or frameshift effects) or untranslated regions (e.g., alteration of mRNA splicing including exonization, or modification in the repartition of the transcripts) [11, 14]. Interestingly, only 10 different LINE-1-mediated insertions of repetitive elements have been reported in six different genes (*ATM*, *BTK*, *CD40LG*, *CYBB*, *FAS*, and *IL2RG)* implicated in PID [11]. The insertion of retrotransposed elements may be underdiagnosed in other PIDs, including MSMD. Screening for such structural variants should be performed in patients with no genetic diagnosis, with a view to the provision of treatment appropriate to the pathophysiology of their disease and genetic counseling for the affected families.

Acknowledgments We thank the patient and his family for their cooperation in this study; Yoann Seeleuthner, Manon Roynard, Bertrand Boisson, Benedetta Bigio, and both branches of the Laboratory of Human Genetics of Infectious Diseases for helpful discussions and support; and Yelena Nemirovskaya, Catherine Heitz, Céline Desvallées, Cécile Patissier, and Dominick Papandrea for administrative support.

Funding The Laboratory of Human Genetics of Infectious Diseases is supported by the National Institute of Allergy and Infectious Diseases grant number 5R37AI095983, the Rockefeller University, the St. Giles Foundation, the French National Institute of Health and Medical Research (INSERM), Paris Descartes University, the Integrative Biology of Emerging Infectious Diseases Laboratory of Excellence (ANR-10-LABX-62-IBEID) and the French National Research Agency under the "Investments for the future" program (grant number ANR-10-IAHU-01), ANR-GENMSMD (grant number ANR-16-CE17-0005-01 for JB) and SRC2017 (for JB). COQ is financially supported by ANR-14-CE15-006-01. JR is financially supported by the INSERM PhD program for medical and pharmaceutical doctors ("poste d'accueil INSERM").

Compliance with Ethical Standards

Statement of Informed Consent Written informed consent was obtained from the guardians of the patient. Informed consent for participation in this study was obtained in accordance with local regulations, with approval from the IRB. The experiments described here were performed in France, in accordance with local regulations, and with the approval of the IRB of Necker Hospital for Sick Children, France.

Conflict of Interest The authors declare that they have no conflict of interest.

References

1. Rosain J, Kong XF, Martinez-Barricarte R, Oleaga-Quintas C, Ramirez-Alejo N, Markle J, et al. Mendelian susceptibility to mycobacterial disease: 2014-2018 update. Immunol Cell Biol. 2019;97(4):360–7.
2. Martinez-Barricarte R, Markle JG, Ma CS, Deenick EK, Ramirez-Alejo N, Mele F, et al. Human IFN-gamma immunity to mycobacteria is governed by both IL-12 and IL-23. Sci Immunol. 2018;3(30). https://doi.org/10.1126/sciimmunol.aau6759
3. Boisson-Dupuis S, Ramirez-Alejo N, Li Z, Patin E, Rao G, Kerner G, et al. Tuberculosis and impaired IL-23-dependent IFN-gamma immunity in humans homozygous for a common TYK2 missense variant. Sci Immunol. 2018;3(30). https://doi.org/10.1126/sciimmunol.aau8714
4. Humblet-Baron S, Franckaert D, Dooley J, Ailal F, Bousfiha A, Deswarte C, et al. IFN-gamma and CD25 drive distinct pathologic features during hemophagocytic lymphohistiocytosis. J Allergy Clin Immunol. 2018;143(6):2215–26.
5. Shabani M, Aleyasin S, Kashef S, Zoghi S, Deswarte C, Casanova JL, et al. A novel recessive mutation of interferon-gamma receptor 1 in a patient with mycobacterium tuberculosis in bone marrow aspirate. J Clin Immunol. 2019;39(2):127–30.
6. Michniacki TF, Walkovich KJ, Frame DG, Vander Lugt MT. Interferon-gamma receptor 1 deficiency corrected by umbilical cord blood transplantation. J Clin Immunol. 2019;39(3):257–60.
7. de Vor IC, van der Meulen PM, Bekker V, Verhard EM, Breuning MH, Harnisch E, et al. Deletion of the entire interferon-gamma receptor 1 gene causing complete deficiency in three related patients. J Clin Immunol. 2016;36(3):195–203.
8. Kutluğ S, Çeliksoy M, Eroğlu B, Yıldız L, Yıldıran A. A case of acute generalised exathematous pustulosis induced by paracetamol. Asthma Allergy Immunol. 2017;15:49–54.
9. Deininger P. Alu elements: know the SINEs. Genome Biol. 2010;12(12):236.
10. Rosain J, Oleaga-Quintas C, Deswarte C, Verdin H, Marot S, Syridou G, et al. A variety of Alu-mediated copy number variations can underlie IL-12Rbeta1 deficiency. J Clin Immunol. 2018;38(5):617–27.
11. Hancks DC, Kazazian HH Jr. Roles for retrotransposon insertions in human disease. Mob DNA. 2016;7:9.
12. Wildschutte JH, Baron A, Diroff NM, Kidd JM. Discovery and characterization of Alu repeat sequences via precise local read assembly. Nucleic Acids Res. 2015;43(21):10292–307.
13. Goerner-Potvin P, Bourque G. Computational tools to unmask transposable elements. Nat Rev Genet. 2018;19:688–704.
14. Payer LM, Steranka JP, Ardeljan D, Walker J, Fitzgerald KC, Calabresi PA, et al. Alu insertion variants alter mRNA splicing. Nucleic Acids Res. 2019;47(1):421–31.